

Supplemental Materials

Molecular Biology of the Cell

Rudkouskaya et al.

SUPPLEMENTAL MATERIALS AND METHODS

Mice and genotyping.

The primers used for genotyping mutant mouse strains were:

Cre: Forward: 5'-CCATCTGCCACCAGCCAG-3', *Cre* reverse: 5'-TCGCCATCTTCCAGCAGG-3',

Cpxm1 forward: 5'-TCGCCATCTTCCAGCAGG-3',

Cpxm1 reverse: 5'-GATGTTGGGGCACTGCTCATTACC-3',

Ilk forward: 5'-CTGTTGCAATACAAGGCTGAC-3',

Ilk reverse: 5'-CTGGGAGAAGCTCTCTAAGGGG-3',

Intb1 forward: 5'-CGGCTCAAAGCAGAGTGTCAGTC-3',

Intb1 reverse: 5'-CCACAACCTTCCCAGTTAGCTCTC-3'.

The amplicon sizes were: *Cre*, 281 bp; *Cpxm1*, 420 bp; *Ilk* floxed, 390 bp, *Ilk* wild type, 360, and *Intb1* floxed, 280 bp, and *Intb1* wild type, 160 bp. Multiplex PCR reactions were prepared to amplify simultaneously *Cre* and *Cpxm1*.

Antibodies and reagents.

Antibodies, their sources and dilutions for immunohistochemistry used are as follows: rabbit anti-aPKC ζ (SC216, Santa Cruz Biotechnology, Santa Cruz, CA, 1:100), β -tubulin (E7, Developmental Studies Hybridoma Bank, developed under the auspices of the NICHD, and maintained by the University of Iowa, Department of Biology, Iowa City, IA, 1:250), mouse anti-ILK (No. 611802, Transduction Laboratories, Lexington, KY, 1:1000), rabbit anti-ILK (No. 3862, Cell Signaling Technology, Danvers, MA, 1:100), rabbit anti-LEF1 (No. 2230, Cell Signaling Technology, Danvers, MA, 1:100), rabbit anti-GSK3- β (No. 51065-1-AP, Proteintech, Chicago, IL, 1:100), rabbit monoclonal anti-phospho-Ser 9 GSK3- β (No. 9323, Cell Signaling Technology, Danvers, MA, 1:100), mouse anti-Keratin 14 (MS-115-P1, Thermo Fisher Scientific, Fremont, CA, 1:100), mouse anti-E-cadherin (No.

334000, Invitrogen, Camarillo, CA, 1:100), rat anti-P-cadherin (No. 13-2000Z, Invitrogen, Camarillo, CA, 1:100), rabbit anti-Laminin $\alpha 5$ chain (a generous gift from Dr. Jeffrey Miner, Washington University School of Medicine, 1:500), rabbit anti-Versican (AB1032, Millipore, Temecula, CA, 1:500), rat anti-CD133 (No. 14-1331, eBioscience, San Diego, CA, 1:100), rabbit anti-Ki67 (ab15580, Abcam, Cambridge, MA, 1:200), rat anti-integrin $\alpha 6$ (555734, BD Biosciences Pharmingen, San Diego, CA, 1:100); rat anti-integrin $\beta 1$ (MAB1997, Millipore, Temecula, CA, 1:100), mouse anti- β -catenin (No. 610154, BD Transduction Laboratories, Franklin Lakes, NJ, 1:500), mouse anti-GATA-3 (sc-268, Santa Cruz Biotechnology, Santa Cruz, CA, 1:100). Alexa Fluor®-conjugated goat anti-mouse or goat anti-rabbit IgG were purchased from Molecular Probes/Invitrogen (Eugene, OR) and were used at a 1:500 dilution. TUNEL assays were conducted with In Situ Cell Detection kits (11684795910, Roche, Mannheim, Germany), following the manufacturer's instructions. Purified laminin-511 was purchased from Biolamina (Stockholm, Sweden). All other chemicals were purchased from Sigma.

In situ hybridization.

In situ hybridization was conducted with 48-mer oligonucleotide probes corresponding to the non-coding strand at positions 1489-1538 within the *Gli1* coding sequence (NM_010296; 5'-ACTGCCTGCTGGGGAGTGGTTCGCTGCTGCAAGAGGACTGCGCTCCGGG-3'). The 3' end FITC-labelled antisense and control sense probes were purchased from GeneDetect (Bradenton, FL). Hybridization of the oligonucleotide probes (200ng/ml, final) to 7- μ m frozen sections was conducted as per manufacturer's instructions. For detection, the probe signal was amplified after post-hybridization washes, by incubation with anti-FITC antibodies conjugated to horseradish peroxidase, followed by amplification using a biotin-tyramide signal amplification kit (TSA Biotin System, Perkin Elmer, Waltham, MA). The specimens were then treated with streptavidin-conjugated horseradish

peroxidase, followed by incubation with ImmPACT NovaRED peroxidase substrate (Vector Laboratories, Burlingame, CA). Tissue sections were counterstained with Methyl Green.

RNA preparation and quantitative reverse-transcription PCR (qPCR).

Total RNA was extracted from dorsal skin of E17.5 mice. RNA quality and quantity were assessed as described (Judah et al, 2012). cDNA was synthesized using SuperScript II (Invitrogen, Carlsbad, CA), and qPCR reactions were conducted on triplicate samples, using QuantiTect SYBR Green kits (Qiagen, Louisville, KY). Triplicate cDNA samples corresponding to 25 ng of initial RNA were amplified using oligonucleotide primer sequences obtained from Primer Search (<http://pga.mgh.harvard.edu/primerbank>), and summarized in Supplemental Table S1. Amplification reactions (40 cycles, 94°C for 15 sec; 60°C for 30 sec, 72°C for 30 sec per cycle) were conducted in a CFX384 Real-Time System (Bio-Rad, Hercules, CA). Separate samples from each of seven *K14Cre;Ilk^{fl+}* and seven *K14Cre;Ilk^{fl}* embryos were used for every transcript assessed. The results were analyzed using CFX Manager 2.0 software (Bio-Rad), and normalized to the expression of the housekeeping genes *Rpl27* and *Rps29*, which encode, respectively, ribosomal protein L27 and S29 (de Jonge et al, 2007). Fold-changes were calculated comparing *K14Cre;Ilk^{fl+}* versus *K14Cre;Ilk^{fl}* tissues, using the $\Delta\Delta C_t$ method.

SUPPLEMENTAL TABLE S1

Primer sequences used for qPCR. The gene accession number is indicated under the name of each transcript shown.

mRNA	FORWARD PRIMER	REVERSE PRIMER
E-cadherin NM_009864	5'-CAGTTCCGAGGTCTACACCTT-3'	5'-TGAATCGGGAGTCTTCCGAAAA-3'
P-cadherin NM_001037809	5'-GCCCAAGTTCACCTCAAGACAC-3'	5'-GTGCCAGGCATTACTCCCTC-3'
Wnt3A NM_009522	5'-CAGGAACTACGTGGAGATCATGC-3'	5'-CGTGTCCTGCGAAAGCTACT-3'
Wnt5A NM_001256224	5'-GGACCACATGCAGTACATTGG-3'	5'-CGTCTCTCGGCTGCCTATTT-3'
Noggin NM_008711	5'-GCCAGCACTATCTACACATCC-3'	5'-GCGTCTCGTTCAGATCCTTCTC-3'
Bmp6 NM_007556	5'-AGAAGCGGGAGATGCAAAGG-3'	5'-GACAGGGCGTTGTAGAGATCC-3'
BmpR1A NM_009758	5'-TGGCACTGGTATGAAATCAGAC-3'	5'-CAAGGTATCCTCTGGTGCTAAAG-3'
Gli1 NM_010296	5'-CCAAGCCAACCTTTATGTCAGGG-3'	5'-AGCCCGCTTCTTTGTTAATTTGA-3'
Rps29 NM_009093	5'-GTCTGATCCGCAAATACGGG-3'	5'-AGCCTATGTCCTTCGCGTACT-3'
Rpl4 NM_024212	5'-CAGACCAGTGCTGAGTCTTGG-3'	5'-TTGGGTTGTATTCACTCTGCG-3'

SUPPLEMENTAL REFERENCES

de Jonge HJ, Fehrmann RS, de Bont ES, Hofstra RM, Gerbens F, Kamps WA, de Vries EG, van der Zee AG, te Meerman GJ, ter Elst A (2007) Evidence based selection of housekeeping genes. *PLoS One* 2: e898

Judah D, Rudkouskaya A, Wilson R, Carter DE, Dagnino L (2012) Multiple roles of integrin-linked kinase in epidermal development, maturation and pigmentation revealed by molecular profiling. *PLoS One* 7: e36704

Duverger O, and Morasso MI (2009) Epidermal patterning and induction of different hair types during mouse embryonic development. *Birth Defects Res (Part C)* 87:263-272.

LEGENDS TO SUPPLEMENTAL FIGURES

Supplemental Figure S1. Schematic of hair follicle morphogenesis. In mice, hair follicle development begins around E14.5, when mesenchymal cells underneath the ectoderm acquire a compact morphology and signal to juxtaposed ectodermal cells, inducing the formation of a stage-1 follicle, or placode. Several signaling molecules are involved in placode formation, including those in the WNT pathway. Subsequent reciprocal signals between the placode and the dermal condensate induce proliferation of the epithelial cells and invagination into the underlying mesenchyme at E15.5. At this stage, Sonic Hedgehog (SHH) pathways become activated in the epithelial cells of the developing follicle, thus inducing further growth to stage-2 (hair germ). A second wave of WNT signaling occurs at E15.5-E16.5, which promotes formation of the hair peg (stage 3-4), in which the dermal condensate forms compact dermal papilla cells. At this stage, the epithelial cells further invaginate into the underlying mesenchyme, and begin to surround the dermal papilla. Inductive signals between the epithelium and the dermal papilla continue, promoting further hair follicle maturation. Matrix progenitor cells, which surround and are adjacent to the dermal papilla, are specified at this stage. Matrix progenitors subsequently mature, giving rise to the matrix and the precortex cells, present in more developed bulbous peg follicles (stages 5-10). A completely developed hair follicle is composed of multiple layers of keratinocytes, which include the outermost Outer Root Sheath (ORS). The ORS surrounds the Inner Root Sheath (IRS), which forms a tube inside of which the hair shaft develops and grows outward. A fully formed follicle also contains sebaceous glands and the bulge area, which constitutes a keratinocyte stem cell niche. Other signaling molecules involved in hair follicle morphogenesis include bone morphogenetic factor, Notch1/Delta1, Eda/Edar, and fibroblast growth factor (Duverger and Morasso, 2009).

Supplemental Figure S2. Abnormal hair follicle morphogenesis in ILK-deficient epidermis.

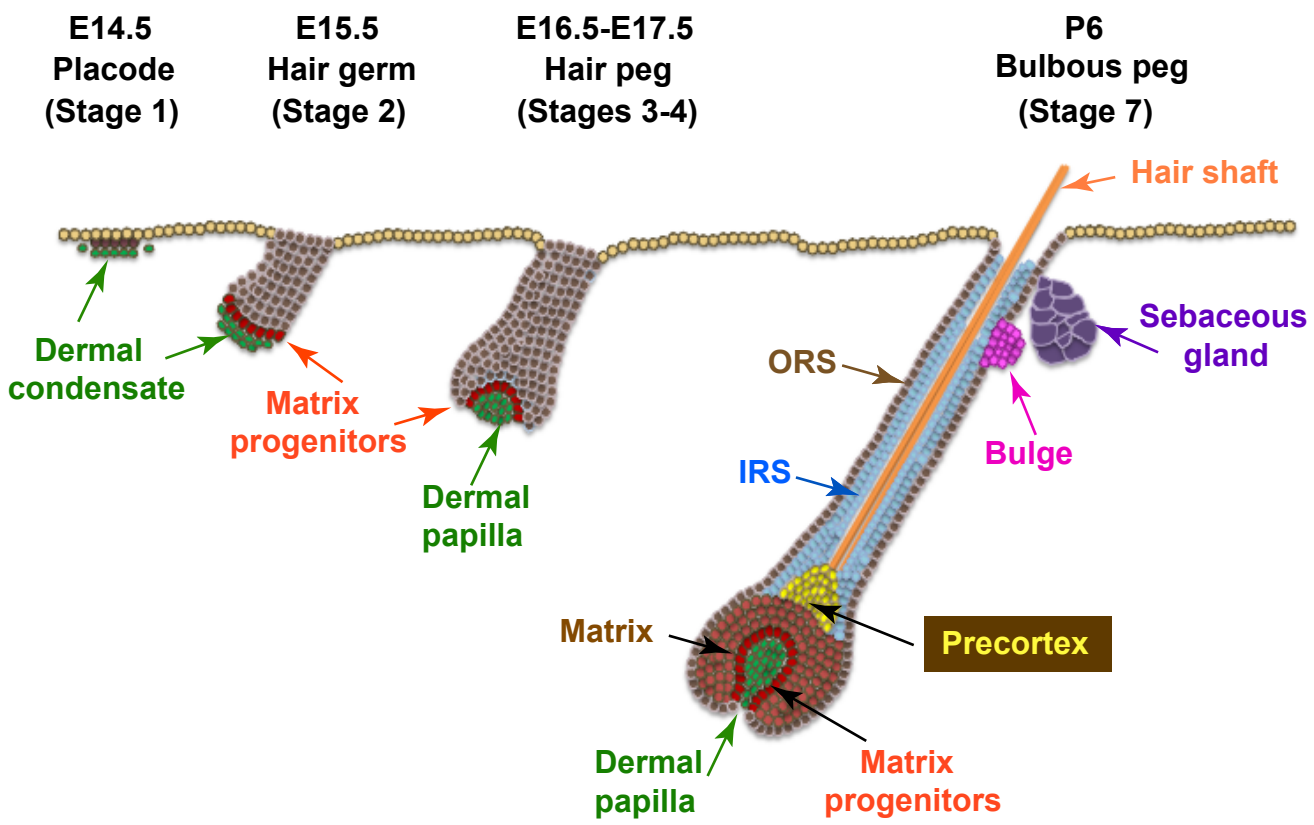
(A) Dorsal epidermal sections from E19.5 mice with the indicated genotype were processed for immunofluorescence microscopy using an anti-ILK antibody. Nuclear DNA was visualized with Hoechst 33342. Filled and dashed lines represent, respectively, the top of the stratum corneum and the dermoepidermal junction. Bar, 32 μm . (B) Quantification of hair follicles in *K14Cre;Ilk^{fl/+}* (gray bars) and *K14Cre;Ilk^{fl/fl}* (black bars) embryos of the indicated gestational ages. Asterisks indicate $P < 0.05$ (Student's t test) (C) Hair follicles in the tissue sections from (B) were staged and quantified. The results are expressed as the percentage of hair follicles at each stage (with 100% corresponding to total hair follicles in each embryo genotype) plus SEM, relative to corresponding hair follicle stages in ILK-expressing versus ILK-deficient embryos within the same gestational age. Asterisks indicate $P < 0.05$, relative to ILK-expressing follicles at the corresponding developmental stage (ANOVA, $n=5$).

Supplemental Figure S3. Signaling pathways altered in ILK-deficient hair follicles.

(A) Dorsal epidermal sections from embryos of the indicated gestational age and genotype were processed for immunofluorescence microscopy using an anti-LEF1 antibody. Nuclear DNA was visualized with Hoechst 33342. Insets represent higher magnification images of boxed areas. Bar, 32 μm . (B) RNA was isolated from the dorsal skin of *K14Cre;Ilk^{fl/+}* and *K14Cre;Ilk^{fl/fl}* E17.5 embryos, and subjected to amplification using quantitative, real-time PCR. The results are expressed as the percentage of indicated transcripts in *K14Cre;Ilk^{fl/fl}* skin, relative to levels in *K14Cre;Ilk^{fl/+}* skin (set to 100%), and are shown as the mean + SEM ($n=7$). The asterisks indicate $P < 0.05$, relative to abundance in *K14Cre;Ilk^{fl/+}* skin (Student's t test). (C) Protein lysates were prepared from dorsal skin (P-cadherin) or epidermis isolated from dorsal skin (ILK) of 3 day-old mice with the indicated genotypes (four different animals

per genotype, obtained from two litters). The lysates were resolved by SDS-PAGE and analyzed by immunoblot with the indicated antibodies. β -tubulin was used to normalize for protein loading. **(D)** Dorsal epidermal sections from embryos of the indicated gestational age and genotype were processed for *in situ* hybridization using antisense probes for *Gli1* mRNA, as summarized in “Materials and Methods”. The sections were counterstained with methyl green. Bar, 50 μ m.

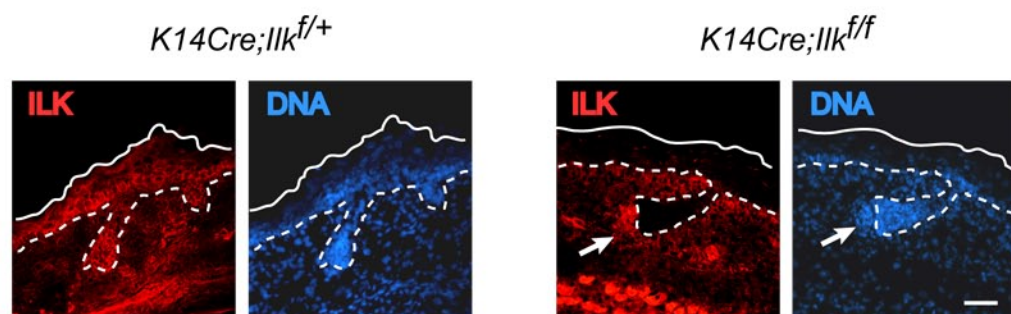
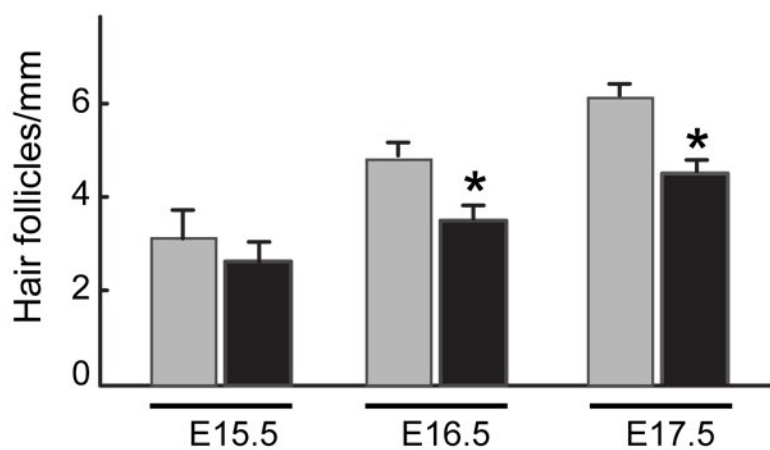
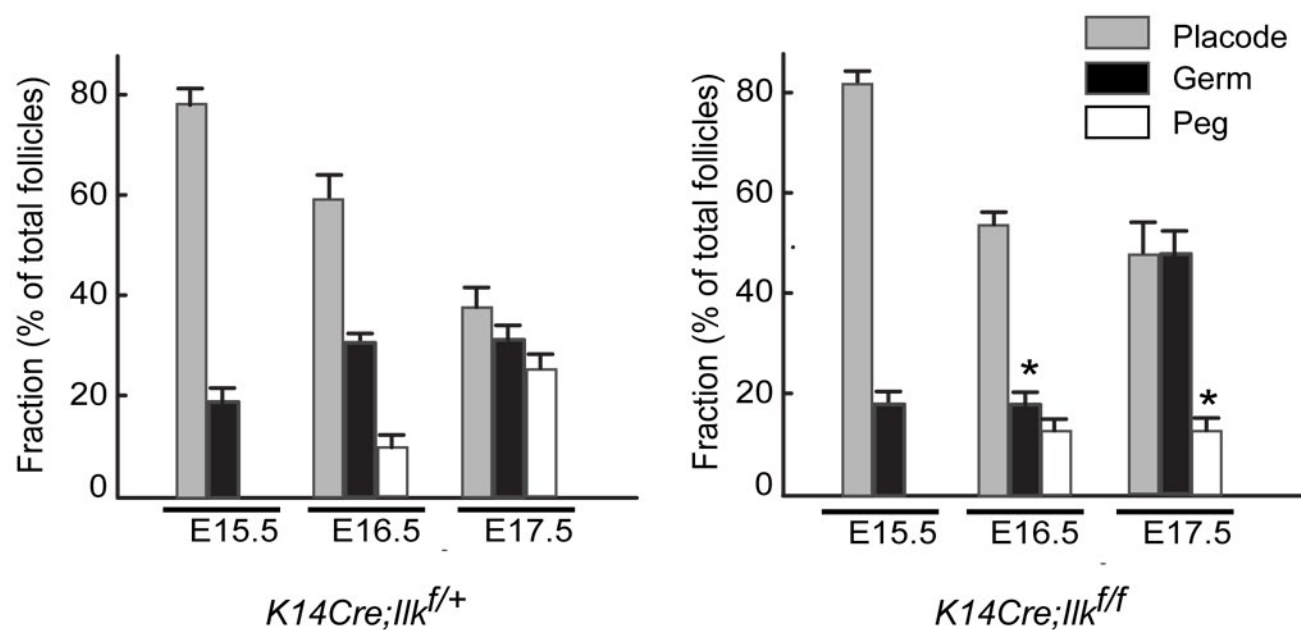
Supplemental Figure S4. Abnormal deposition of laminin-511 in integrin β 1-deficient hair follicles. Dorsal epidermal sections from E17.5 embryos of the indicated genotype were processed for immunofluorescence microscopy using antibodies against laminin-511 and CD133. Nuclear DNA was visualized with Hoechst 33342. Arrows represent the lowermost portion of the developing hair follicle, shown at higher magnification in the photomicrographs at the bottom. Bar, 50 μ m.

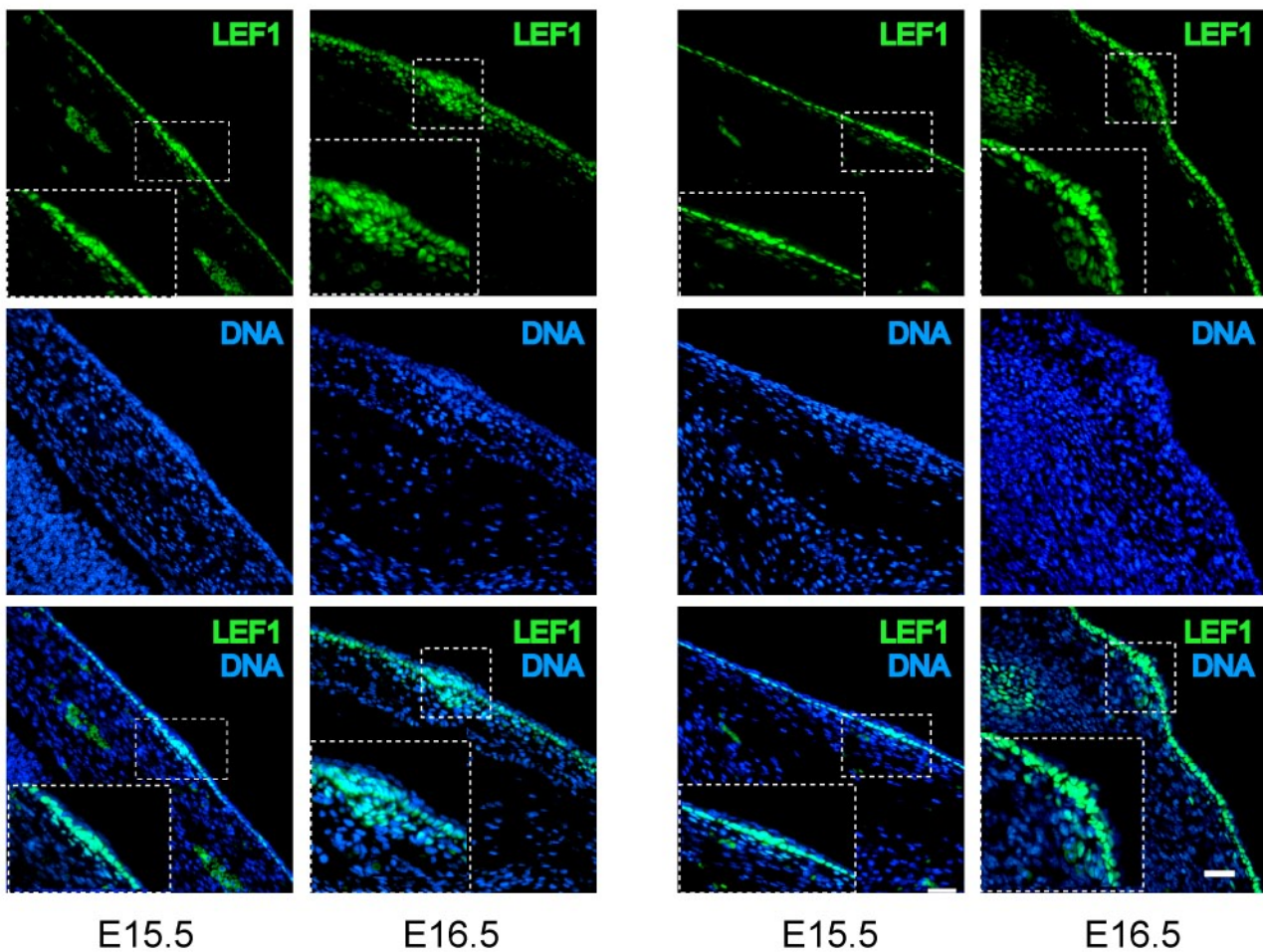


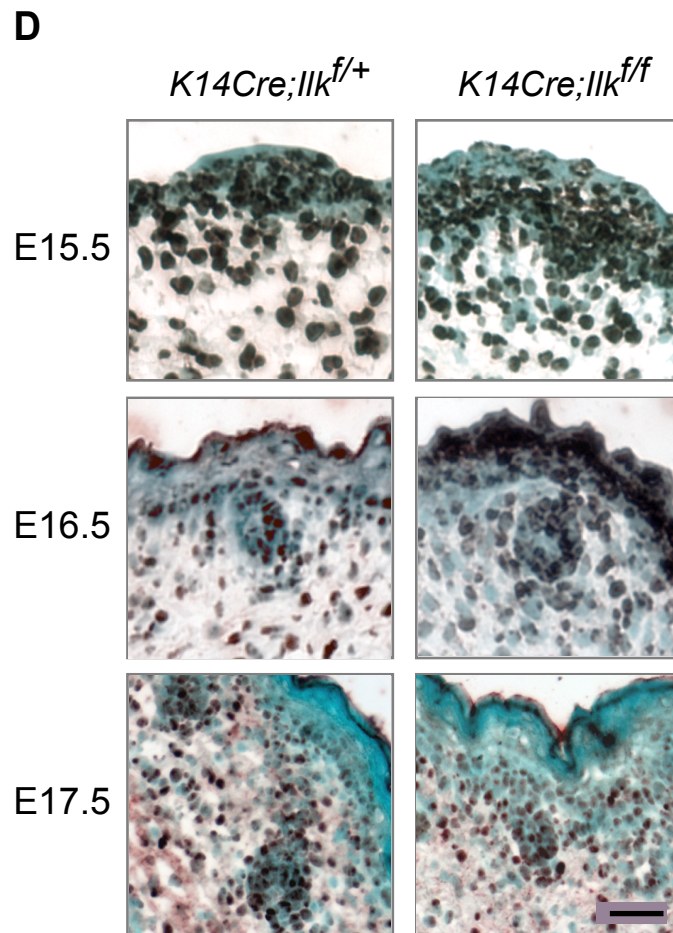
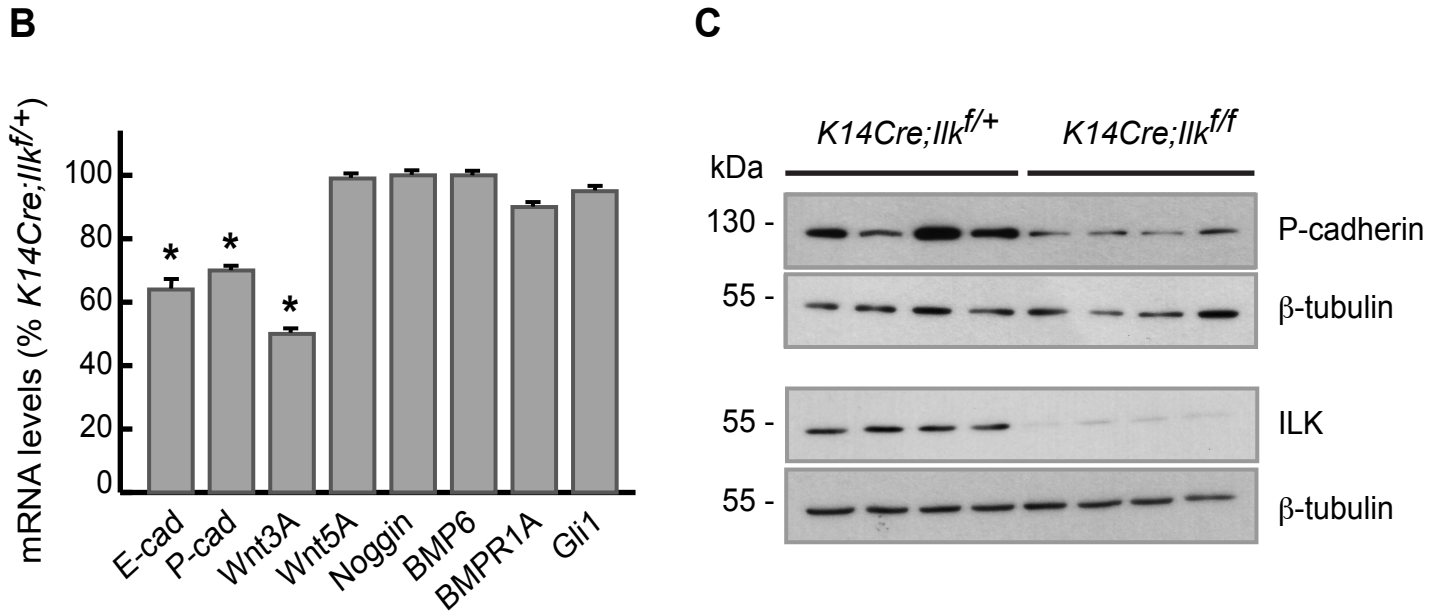
WNT

SHH, BMP

Supplemental Figure S1

A**B****C**

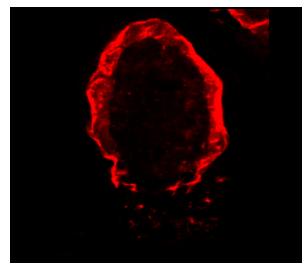
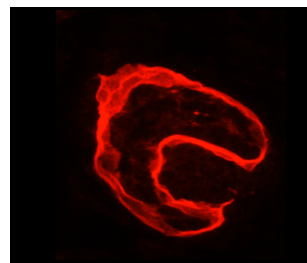
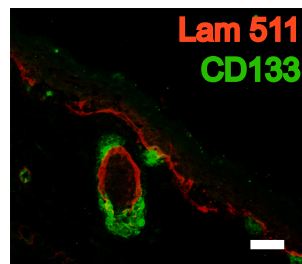
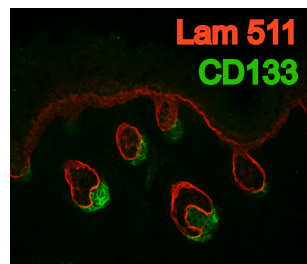
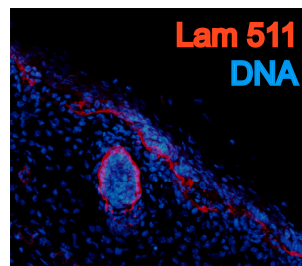
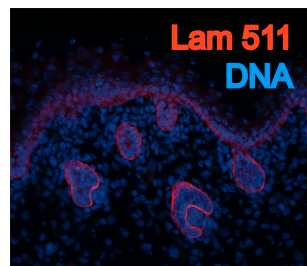
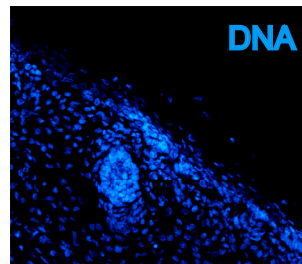
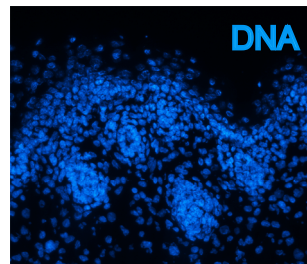
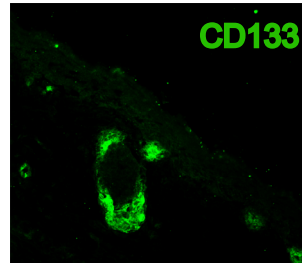
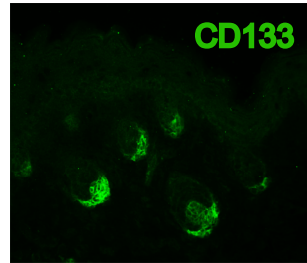
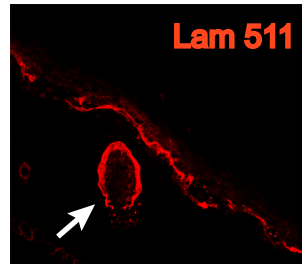
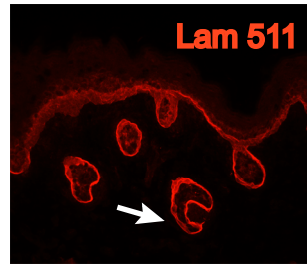
A*K14Cre;Ilk^{f/+}**K14Cre;Ilk^{f/f}*



Supplemental Figure S4

K14Cre;Intb1^{f/+}

K14Cre;Intb1^{f/f}



Supplemental Figure S5